is worthwhile to mention that the synthetic route reported herein is flexible enough to prepare aplysiatoxins with modified acid side chains in order to investigate the structure–activity relationships; indeed, all the possible stereoisomers with respect to the C.29 and C.30 positions of debromoaplysiatoxin have successfully been obtained by using the same sequence of reactions.

Acknowledgment. Financial support from the National Institutes of Health (CA-22215) is gratefully acknowledged. C.A.B. thanks the National Institutes of Health for the support of a Postdoctoral Fellowship (GM-38051).

Supplementary Material Available: Experimental details for the synthesis of **3**, **4**, and **7** and ^{1}H NMR spectra of key intermediates (26 pages). Ordering information is given on any current masthead page.

---

(19) For recent reviews and papers on this subject, see, for example: (a) *Carcinogenisis: Mechanisms of Tumor Promotion and Cocarcinogenesis*; Slaga, T. J., Sivak, A., Boutwell, R. K., Eds.; Raven: New York, 1978. (b) *Cellular Interactions by Environmental Tumor Promoters*; Fujiki, H., Hecker, E., Moore, R. E., Sugimura, T., Eds.; Japan Science Society Press: Tokyo, 1984. (c) *Biochemical Basis of Chemical Carcinogenesis*; Greim, H., Jung, R., Kramer, M., Marquardt, H., Oesch, F., Eds.; Raven: New York, 1984. (d) Jeffrey, A. M.; Liskamp, R. M. J. *Proc. Natl. Acad. Sci. U.S.A.* **1986**, *83*, 241. (e) Wender, P. A.; Koehler, K. F.; Sharkey, N. A.; Dell'Aquila, M. L.; Blumberg, P. M. *Proc. Natl. Acad. Sci. U.S.A.* **1986**, *83*, 4214.

Binuclear Mixed-Valence $\mathrm{Mn^{II}Mn^{III}}$ Complexes: Insight About the Resolution of Hyperfine Structure in the EPR Spectrum

Habibe Diril,[1] Hsiu-Rong Chang,[2] Xiaohua Zhang,[1]
Scott K. Larsen,[3] Joseph A. Potenza,*[1]
Cortlandt G. Pierpont,*[3] Harvey J. Schugar,*[1]
Stephan S. Isied,*[1] and David N. Hendrickson*[2]

Department of Chemistry
Rutgers, The State University of New Jersey
New Brunswick, New Jersey 08903
School of Chemical Sciences
University of Illinois, Urbana, Illinois 61801
Department of Chemistry
University of Colorado, Boulder, Colorado 80309

Received June 10, 1987

A manganese protein containing two to four Mn ions,[4] and possibly other redox components,[4c] serves as the water oxidation center in photosynthesis. Substantial insight regarding the electronic structure of the Mn site has been obtained from an analysis of the hyperfine-structured EPR signal for the S_2 state in photosystem II.[5] Low molecular weight polynuclear Mn complexes that exhibit rich EPR spectra and/or catalytically oxidize water to O_2 are of interest. We report here the first structural characterization of binuclear $\mathrm{Mn^{II}Mn^{III}}$ complexes $[\mathrm{Mn_2(bpmp)}(\mu\text{-OAc})_2](\mathrm{ClO_4})_2\cdot\mathrm{H_2O}$[6] (**1**) and $\mathrm{LMn_2Cl_2Br}$ (**2**) and show how the development of EPR hyperfine structure at low

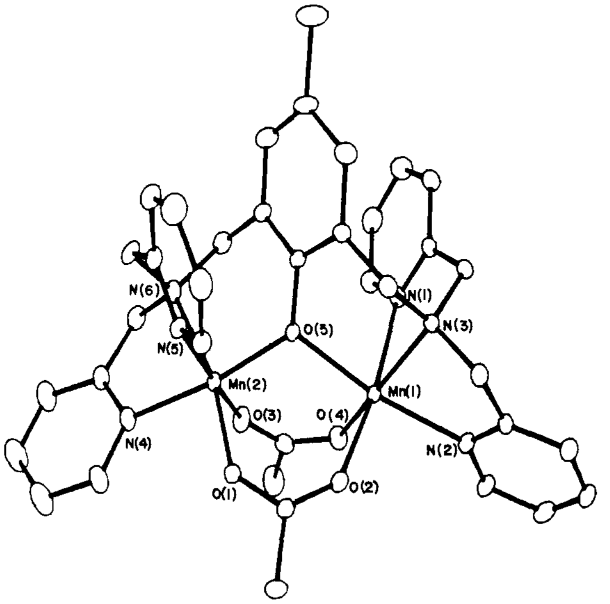

Figure 1. ORTEP plot of $[\mathrm{Mn_2(bpmp)}(\mu\text{-OAc})_2]^{2+}$ in complex **1**. Selected interatomic distances (Å) and angles (deg) are the following: Mn(1)–O(2), 2.166 (4); –O(4), 2.066 (5); –O(5) 2.193 (4); –N(1), 2.271 (6); –N(2), 2.210 (6); –N(3), 2.324 (5). Mn(2)–O(1), 1.927 (5); –O(3), 2.090 (4); –O(5), 1.903 (4); –N(6), 2.073 (5); –N(4), 2.052 (5); –N(5), 2.235 (6); Mn(1)···Mn(2), 3.447 (1). Mn(1)–O(5)–Mn(2), 114.4 (2).

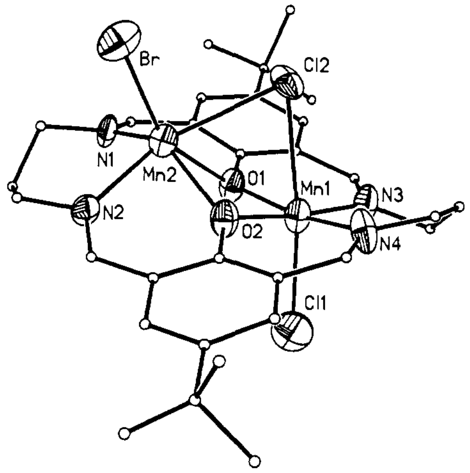

Figure 2. ORTEP plot of $\mathrm{LMn_2Cl_2Br}$ (**2**). The Cl(1) and Br atoms are disordered, see ref 11. Selected interatomic distances (Å) and angles (deg) are the following: Mn(1)–O(1), 1.941 (9); –O(2), 1.931 (10); –N(3), 1.973 (13); –N(4), 2.031 (12); –Cl(1), 2.491 (5); –Cl(2), 2.766 (6). Mn(2)–O(1), 2.386 (11); –O(2), 2.129 (10); –N(1), 2.182 (11); –N(2), 2.236 (12); –Cl(2), 2.763 (5); –Br, 2.514 (4); Mn(1)···Mn(2), 3.168 (3). Mn(1)–O(1)–Mn(2), 93.6 (4); Mn(1)–O(2)–Mn(2), 102.5 (4).

---

(1) Rutgers University.

(2) University of Illinois.

(3) University of Colorado.

(4) (a) Dismukes, G. C. *Photochem. Photobiol.* **1986**, *43*, 99–115. (b) Govindjee; Kambara, T.; Coleman, W. *Photochem. Photobiol.* **1985**, *42*, 187–210. (c) Kambara, T.; Govindjee *Proc. Natl. Acad. Sci. U.S.A.* **1985**, *82*, 6119–6123. (d) Webber, A. N.; Spencer, L.; Sawyer, D. T.; Heath, R. L. *FEBS Lett.* **1985**, *189*, 258–262. (e) Amesz, J. *Biochim. Biophys. Acta* **1983**, 726, 1–12. (f) Livorness, J.; Smith, T. D. *Stuct. Bonding (Berlin)* **1982**, *48*, 2–44. (g) Sauer, K. *Acc. Chem. Res.* **1980**, *13*, 249–256. (h) Radmer, R.; Cheniae, G. In *Topics in Photosynthesis*; Barber, J., Ed.; Elsevier: Amsterdam, 1977.

(5) (a) Dismukes, G. C.; Siderer, Y. *Proc. Natl. Acad. Sci. U.S.A.* **1981**, *78*, 274–278. (b) Hansson, O.; Andreasson, L.-*E. Biochim. Biophys. Acta* **1982**, *679*, 261–268. (c) Brudvig, G. W.; Casey, J. L.; Sauer, K. *Biochim. Biophys. Acta* **1983**, *723*, 366–371. (d) de Paula, J. C.; Beck, W. F.; Brudvig, G. W. *J. Am. Chem. Soc.* **1986**, *108*, 4002–4009. (e) de Paula, J. C.; Innes, J. B.; Brudvig, G. W. *Biochemistry* **1985**, *24*, 8114–8120. (f) Zimmermann, J.–L.; Rutherford, A. W. *Biochemistry* **1986**, *25*, 4609–4615. (g) Hansson, Ö.; Aasa, R.; Vänngärd, T. *Biophys. J.* **1987**, *51*, 825–832.

(6) (a) A preliminary account of the preparation, structure, and detailed characterization of this complex was presented at the 192nd National Meeting of the American Chemical Society, Anaheim, CA (Sept. 1986, Inorg. 205). A somewhat overlapping study of the same complex was reported by Suzuki et al. (*Chem. Lett.* **1987**, 281–184) while this manuscript was being prepared. (b) The structure of the polymeric $\mathrm{Mn^{II}Mn^{III}}$ complex $[\mathrm{Me_4N}][\mathrm{Mn_2(CN)_6}]\cdot 8\mathrm{H_2O}$ with low-spin $\mathrm{Mn^{III}(CN)_6}$ and high-spin $\mathrm{Mn^{II}(H_2O)_4(NC)_2}$ moieties has been reported, see: Babel, D.; Kurtz, W. *Stud. Inorg. Chem.* **1983**, *3*, 593. (c) The structure and properties of a related binuclear $\mathrm{Mn_2}^{\mathrm{III}}$ complex have been reported, see: Sheats, J. E.; Czernuszewicz, R. S.; Dismukes, G. C.; Rheingold, A. L.; Petrouleas, V.; Stubbe, J.; Armstrong, W. H.; Beer, R. H.; Lippard, S. J. *J. Am. Chem. Soc.* **1987**, *109*, 1435–1444.

0002-7863/87/1509-6207$01.50/0

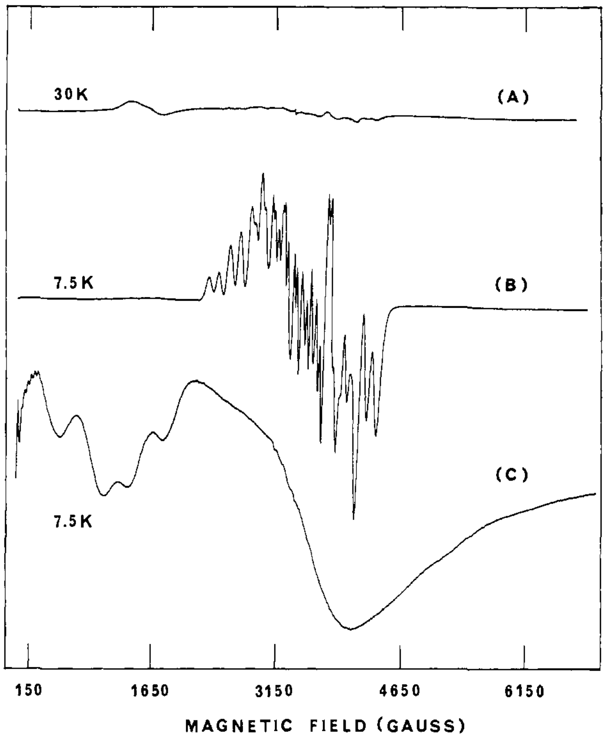

Figure 3. X-band EPR spectra. Traces A and B are for an acetone/toluene/ethanol glass of $[Mn_2(bpmp)(\mu\text{-}OAc)_2](ClO_4)_2{\cdot}H_2O$ (**1**) at 30 and 7.5 K, respectively. Trace C is for LMn_2Cl_2Br (**2**) at 7.5 K in a dichloromethane/toluene glass.

temperature relates to the strength of the Mn···Mn magnetic coupling. The ligands $bpmp^-$ and L^{2-} are

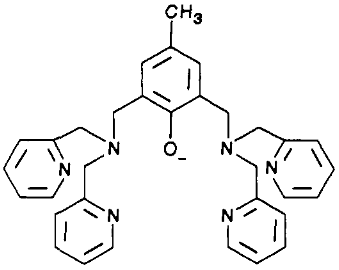

$(bpmp^-)$[7]

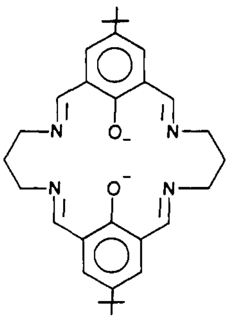

(L^{2-})[8]

Compound **1** was prepared by air oxidation of a complex formed from $Mn(OAc)_2$ and $bpmp^-$ and crystallized as the perchlorate salt; **2** was prepared by oxidation of LMn_2Cl_2 with bromine water.[9] X-ray analysis[10] of **1** revealed binuclear $[Mn_2(bpmp)(\mu\text{-}OAc)_2]^{2+}$ cations (Figure 1) in which each Mn ion is bridged by two acetate O atoms and the phenoxy O atom of $bpmp^-$. Mn(1) has metal–ligand distances typical of Mn^{II} and has a distorted octahedral coordination geometry. Mn(2), designated as Mn^{III}, clearly shows the relatively short equatorial and long axial [Mn(2)–O(3), –N(5)] distances characteristic of Jahn–Teller distorted six-coordinate Mn^{III}.

X-ray analysis[11] of **2** also indicates a valence-trapped $Mn^{II}Mn^{III}$ complex (Figure 2); in this case, Mn(1) is a Jahn–Teller distorted Mn^{III} ion while the Mn^{II} ion (Mn(2)) shows trigonal prismatic coordination. The Mn ions are bridged by Cl(2) and phenoxide O atoms O(1) and O(2).

Magnetic susceptibility data for **1** (μ_{eff}/complex = 7.13 μ_B at 298 K to 1.76 μ_B at 2.2 K) are consistent with isotropic magnetic exchange between high-spin Mn^{II} and Mn^{III} ions with $J = -6.0$ cm^{-1}. Corresponding data for **2** (7.82 μ_B at 300 K to 4.48 μ_B at 6 K) gave $J = -1.7$ cm^{-1}.

The EPR spectra for glassed **1** exhibit a dramatic temperature dependence (Figure 3). Above ~15 K, there is a broad $g \sim 4$ signal which is likely attributable to complexes in the $S = {}^3/_2$ state. At 30 K, a hyperfine-structured $g \sim 2$ signal is barely visible; this signal becomes prominent at 15 K and, finally, at 7.5 K, at least 29 Mn hyperfine lines are resolved. The $g \sim 2$ signal is rhombic and arises from the $S = {}^1/_2$ ground state of **1**. Each Mn ion in this valence-trapped complex has a unique **A** tensor. Efforts to simulate[12] the EPR signal assuming collinear **A** tensors for Mn(1) and Mn(2) were not successful, in agreement with the low site symmetry of **1**.

In contrast to **1**, the EPR spectra of glassed **2** or isostructural LMn_2Br_3 (Figure 3) show only broad features and little hyperfine resolution at temperatures down to 7.5 K. Owing to the small exchange coupling ($J = -1.7$ cm^{-1}), the hyperfine structure of the $S = {}^1/_2$ ground state (33% occupancy) has been obscured by relaxation effects and superpositions of signals from the ${}^3/_2$, ${}^5/_2$, ${}^7/_2$, and ${}^9/_2$ excited states (occupancy = 25%, 20%, 13%, and 9%, respectively).

To obtain reliable and unique simulations for the EPR spectra of these complexes, experiments at frequencies other than X-band and single-crystal studies are in progress.

Acknowledgment. We are thankful for support from National Institutes of Health Grant HL 13652 (D.N.H.), The Rutgers research council (S.S.I.), 1510 RR01486 01A1 (crystallographic instrumentation at Rutgers, H.J.S.), and National Science Foundation Grants CHE 85-03222 (C.G.P.) and CHE 84-12182, the last of which partially financed X-ray instrumentation at the University of Colorado.

Supplementary Material Available: Positional and thermal parameters for $[Mn_2(bpmp)(\mu\text{-}OAc)_2](ClO_4)_2{\cdot}H_2O$ (**1**) and LMn_2Cl_2Br (**2**) (11 pages). Ordering information is given on any current masthead page.

---

(7) Suzuki, M.; Kanatomi, H.; Murase, I. *Chem. Lett., Chem. Soc. Jpn.* **1981**, 1745–1748.

(8) This is a Robson-type ligand: Pilkington, N. H.; Robson, R. *Aust. J. Chem.* **1970**, *23*, 2225.

(9) Complexes **1** and **2** gave good elemental analyses.

(10) Crystallography: $Mn_2O_5N_6C_{37}H_{39}{\cdot}2ClO_4{\cdot}H_2O$, monoclinic, $P2_1/n$, $a = 12.493$ (1) Å, $b = 21.583$ (2) Å, $c = 16.631$ (2) Å, $\beta = 95.31$ (1)°, $V = 4465$ (1) Å^3, $Z = 4$; $d_{obsd} = 1.44$ (1) g/cm^3, $d_{calcd} = 1.450$ g/cm^3. The structure was solved by direct methods with 4298 unique reflections ($I > 3\sigma(I)$) collected at 297 (1) K with Mo Kα radiation ($\lambda = 0.71073$ Å to $2\theta = 45°$ on an Enraf-Nonius CAD-4 diffractometer). All atoms of the $Mn_2O_5N_6C_{37}H_{39}$ dication were located and refined, except for methyl group H atoms that were not included. In the cation, non-H atoms were refined anisotropically while H atom coordinates were refined isotropically. Both the perchlorate anions and the solvate water molecule showed large thermal parameters and/or disorder. One perchlorate group was modeled assuming disorder about a threefold axis (6 partially occupied sites for 3 O atoms). Refinement, with the O atoms of the perchlorate and water groups isotropic, yielded $R = 0.061$, $R_w = 0.085$ and G.O.F. = 2.82. The largest peak in a final difference map was 0.77 e/Å^3.

(11) Crystallography: $Mn_2C_{30}H_{38}N_4O_2Cl_2Br{\cdot}H_2O$, monoclinic, $C2/c$, $a = 21.064$ (4) Å, $b = 13.559$ (4) Å, $c = 27.652$ (6) Å, $\beta = 105.51$ (2)°, $V = 7609.3$ Å^3 at 295 *K*, $d_{calcd} = 1.336$ g cm^{-3}, $d_{obsd} = 1.38$ (3) g cm^{-3}, $Z = 8$, $R = 0.071$, $R_w = 0.097$ for 1732 observed reflections ($F > 6\sigma(F)$). Both tertiary butyl groups and one trimethylene group were disordered. The trimethylene group was modeled assuming two half-occupied sites for each C atom. In addition, the terminal halogen atoms were disordered. The atom shown in Figure 2 as Cl(1) was located at a site occupied by ${}^1/_3$ Br and ${}^2/_3$ Cl ions, while that labeled Br was located at a ${}^2/_3$ Br, ${}^1/_3$ Cl position. For each disordered halogen site, independent temperature factors were refined, but the coordinates for Br and Cl were constrained to be the same. Relaxation of this constraint led to singular matrices. The broad EPR spectra of **2** do not result from these disorders. Similarly, broad EPR spectra are exhibited by the all-bromine analogue of **2**. Numerous examples exist of well-resolved EPR spectra of glassed samples containing fluxional rings or *tert*-butyl groups frozen in several conformations.[13]

(12) The same computer program was used as we described before: Mabad, B.; Tuchagues, J.-P.; Hwang, Y. T.; Hendrickson, D. N. *J. Am. Chem. Soc.* **1985**, *107*, 2801.

(13) (a) Long, R. C.; Hendrickson, D. N. *J. Am. Chem. Soc.* **1983**, *105*, 1513. (b) Hendrickson, D. N.; Long, R. C.; Hwang, Y. T.; Chang, H.-R. In *Biological & Inorganic Copper Chemistry*; Karlin, K. D., Zubieta, J., Eds.; Adenine Press: Guilderland, New York, 1986.